

# Dynamics of the Magnetic Flux Trapped in Fractal Clusters of a Normal Phase in Superconductor

Yu. I. Kuzmin

*Ioffe Physical Technical Institute of Russian Academy of Sciences,*

*Polytechnicheskaya 26 St., Saint Petersburg 194021 Russia*

*e-mail: yurk@shuv.ioffe.rssi.ru; iourk@usa.net*

*tel.: +7 812 2479902; fax: +7 812 2471017*

(December 2, 2024)

The influence of geometry and morphology of superconducting structure on critical currents and magnetic flux trapping in percolative type-II superconductor is considered. The superconductor contains the clusters of a normal phase, which act as pinning centers. It is found that such clusters have significant fractal properties. The main features of these clusters are studied in detail: the cluster statistics is analyzed; the fractal dimension of their boundary is estimated; the distribution of critical currents is obtained, and its peculiarities are explored. It is examined thoroughly how the finite resolution capacity of the cluster geometrical size measurement affects the estimated value of fractal dimension. The effect of fractal properties of the normal phase clusters on the electric field arising from magnetic flux motion is investigated. The voltage-current characteristics of superconductors in the resistive state for an arbitrary fractal dimension are obtained. It is revealed that the fractality of the boundaries of the normal phase clusters intensifies the magnetic flux trapping and thereby raises the critical current of a superconductor.

## I. INTRODUCTION

An important property of the clusters of a normal phase in superconductor consists in their capability to trap a magnetic flux. By virtue of their capacity to hold the vortices from moving under the action of the Lorentz force, such clusters can act as effective pinning centers [1]- [5]. This feature is used widely in the making new composite superconducting materials of high current-carrying capability [6], [7]. The morphological characteristics of clusters of a normal phase exert an appreciable effect on magnetic flux dynamics in superconductors, especially when the clusters have fractal boundaries [8]- [10]. In the present work the geometric probability properties of such fractal clusters are considered in detail, and their influence on the dynamics of trapped magnetic flux and critical currents is analyzed.

The further consideration will be concerned with the superconductor containing inclusions of a normal phase, which are out of contact with one another. Let us assume that these inclusions are oriented in such a way that their extent along one of directions far exceeds other linear sizes. The similar columnar defects are of most interest for creating the artificial pinning centers [6], [10]- [14]. When such a superconducting structure is cooled below the critical temperature in the magnetic field along the direction of the longest size of these inclusions, the magnetic flux will be frozen in the normal phase clusters. Even after the external field has been turned off, the flux trapped in these clusters is kept unchanged due to the currents that are steadily circulating around them through the superconducting loops. The distribution of the trapped magnetic flux resulting from such a magnetization in the field-cooling regime will be two-dimensional. The similar distribution can readily be realized in the superconducting film where the normal phase inclusions are created during the growth process at the sites of defects on the boundary with the substrate in such a way that their orientation is normal to the surface of the film [6], [13], [14]. Let us suppose that the film surface fraction covered by the normal phase is below the percolation threshold for the transfer of magnetic flux (50 % for 2D- percolation [15]). In this case the relative portion of superconducting phase exceeds the percolation threshold, so there is a superconducting percolation cluster in the plane of the film where a transport current can flow. Such a structure provides for effective pinning and thereby raises the critical current, because the magnetic flux is locked in finite clusters of a normal phase, and so the vortices cannot leave them without crossing the surrounding superconducting space. If the transport current is passed through the sample, the trapped magnetic flux remains unchanged as long as the vortices are still held in the normal phase clusters. When the current is increased, the magnetic flux starts to break away from the clusters of pinning force weaker than the Lorentz force created by the transport current. As this takes place, the vortices will first pass through the weak links, which connect the normal phase clusters between themselves. Such weak links form especially readily in high-temperature superconductors (HTS) characterized by an extremely short coherence length. Various structural defects, which would simply cause some additional scattering at long coherence length, give rise to the weak links in HTS. There is a hierarchy of weak links over a wide range of scales in HTS [6], [16]- [24]. At an atomic level the weak links are formed by the structural atomic defects, primarily, by oxygen vacancies [18], [25]. On a mesoscopic scale twin boundaries are mainly responsible for weak links existence [18]- [21], [26]. The twins can be spaced up to several nanometers apart, so even single crystal has fine substructure caused by twins. At last, on a macroscopic scale there are manifold structural defects which can form weak links: that may be grain or crystallite boundaries as well as barriers arising from the secondary degrading the non-stoichiometric crystal into the domains with a high and low content of oxygen [22]- [24].

Moreover, a magnetic field further reduces a coherence length [27], thus resulting in more easy weak links formation. In conventional low-temperature superconductors, which are characterized by a large coherence length, the weak links can be formed due to the proximity effect in sites of minimum distance between the next normal phase clusters.

As soon as the transport current is turned on, this one is added to all the persistent currents, which maintain the magnetic flux trapped. Each of these currents is circulating through the superconducting loop around the normal phase cluster wherein the corresponding portion of the magnetic flux is trapped. The loop contains weak links that join the adjacent normal phase clusters transversely to the path of the current. As the transport current is increased, there will come a point when the overall current flowing through the weak link will exceed the critical value, so this link will turn into a resistive state. As this takes place, the space distribution of the currents throughout the superconducting cluster is changed in such a way that the resistive subcircuit will be shunted by the superconducting paths where weak links are not damaged yet. Magnetic field created by this re-distributed transport current acts via the Lorentz force on the current circulating around the normal phase cluster. As a consequence, the magnetic flux trapped therein will be forced out through the resistive weak link, which has become permeable to the vortices.

## II. FRACTAL GEOMETRY OF NORMAL PHASE CLUSTERS

Thus, whatever the microscopic nature of weak links may be, they form the channels for vortex transport where the pinning force is weaker than the Lorentz force created by the transport current. It appears that according to their configuration each normal phase cluster has its own value of the critical current of depinning, which contributes to the overall statistical distribution. When a transport current is gradually increased, the vortices will break away first from clusters of small pinning force, and therefore, of small critical current. Thus the decrease in the trapped magnetic flux  $\Delta\Phi$  is proportional to the number of all the normal phase clusters of critical currents less than a preset value  $I$ . Therefore, the relative decrease in the trapped flux can be expressed with the cumulative probability function  $F = F(I)$  for the distribution of the critical currents of clusters:

$$\frac{\Delta\Phi}{\Phi} = F(I) \quad , \quad \text{where} \quad F(I) = \Pr \{ \forall I_j < I \} \quad (1)$$

The right-hand side of Eq. (1) is the probability that any  $j$ -th cluster has the critical current  $I_j$  less than a given upper bound  $I$ .

On the other hand, the magnetic flux trapped into a single cluster is proportional to its area  $A$ , so the decrease in the total trapped flux can be represented by the cumulative probability function  $W = W(A)$  for the distribution of the areas of the normal phase clusters, which is a measure of the number of the clusters of area smaller than a given value of  $A$ :

$$\frac{\Delta\Phi}{\Phi} = 1 - W(A) \quad , \quad \text{where} \quad W(A) = \Pr \{ \forall A_j < A \} \quad (2)$$

The distribution function  $W = W(A)$  of the cluster areas can be found by the geometric probability analysis of electron photomicrographs of superconducting films [13]. So, in the practically important case of thick YBCO films containing columnar defects [13], [14] the exponential distribution can be realized:

$$W(A) = 1 - \exp\left(-\frac{A}{\bar{A}}\right) \quad (3)$$

where  $\bar{A}$  is the mean area of the cluster.

Thus, in order to clear up how the transport current acts on the trapped magnetic flux, it is necessary to find out the relationship between the distribution of the critical currents of the clusters (Eq. (1)) and the distribution of their areas (Eq. (2)). The larger the cluster size, the more weak links rise from its perimeter bordering with the surrounding superconducting space, and therefore, the smaller is the critical current at which the magnetic flux breaks away from this cluster. On the basis of this simple geometric argument, let us suppose that this critical current  $I$  is inversely proportional to the perimeter  $P$  of the normal phase cluster:  $I \propto 1/P$ , because the larger the perimeter is, the higher is the probability to get a weak link there. At this point it is assumed that the weak link concentration per unit perimeter length is constant for all clusters and all the clusters of equal perimeter have the same pinning force. Also suppose that after the vortex enters the weak link, it will pass all the way between two adjacent normal phase clusters without being trapped. Here, the magnetic flux is transferred by Josephson vortices. The Josephson penetration depth is large enough in the considered materials, so the size of the region, where the vortex is localized, much exceeds the characteristic length of all possible structural defects that can occur along the transport channel. Thus the probability that such a vortex will be trapped in passing through a weak link under the action of the Lorentz force is very small.

Thus, to deal with the distribution function of Eq. (1), the relation between perimeter and area of clusters should be studied. As has been first found in Ref. [10], the fractal nature of the normal phase clusters exerts an appreciable effect on the dynamics of a magnetic flux in superconductors. For fractal clusters a relation between perimeter and area has the form:

$$P \propto A^{\frac{D}{2}} \quad (4)$$

where  $D$  is the fractal dimension of the cluster perimeter (so-called coastline dimension) [28].

The relation of Eq. (4) is consistent with the generalized Euclid theorem [28], [29], which states that the ratios of the corresponding measures are equal when reduced to the same dimension. Hence it follows that  $P^{1/D} \propto A^{1/2}$ , which is valid both for Euclidean ( $D = 1$ ), and for fractal clusters ( $D > 1$ ).

The fractal dimension value can be estimated by means of regression analysis of the sampling of the areas and perimeters of the normal phase clusters. Such geometric probability analysis was carried out by the procedure described in Ref. [10]. For this purpose an electron photomicrograph of YBCO film, which was similar to that published earlier in Ref. [14], has been scanned. The perimeters and areas of clusters have been measured by covering their digitized pictures with a square grid of spacing  $60 \times 60 \text{ nm}^2$ . The results of the statistical treatment of these data are presented in Table I. The normal phase has occupied 20% of the total surface only, so the transport current can flow through the sufficiently dense percolation superconducting cluster. The primary sampling has contained 528 normal phase clusters located on the scanned region of a total area of  $200 \mu\text{m}^2$ . The distribution of the cluster areas is fitted well to exponential cumulative probability function of Eq. (3) with the mean cluster area  $\bar{A} = 0.0765 \mu\text{m}^2$ . All the points of the primary sampling are marked by crosses on the plot 1 of Fig. 1, which shows the perimeter-area relation for the normal phase clusters. Figure 1 also demonstrates such an important peculiarity of this relation: the scaling law of Eq. (4) is valid in the range of almost three orders of magnitude in cluster area. The scaling perimeter-area behavior means that there is no characteristic length scale between  $0.1 \mu\text{m}$  and  $10 \mu\text{m}$  in the linear size of the normal phase cluster. Whatever the shape and size of the clusters may be, all the points fall closely on the same straight line in logarithmic scale; so that there are no apparent kinks or crossovers on the graph. This enables the fractal dimension  $D$  of the cluster perimeter to be estimated from the slope of the regression line of the form of Eq. (4), thus a least squares treatment of the perimeter-area data for the primary sampling gives the estimate of  $D = 1.44 \pm 0.02$  with correlation coefficient 0.929.

This point that the found value of coastline fractal dimension differs appreciably from unity engages a great attention. What this means is that the fractal properties of the cluster boundary are of prime importance here. Two straight lines (5) in Fig. 1 bound the range of the slopes that the dependencies of the perimeter on the cluster area can have for any arbitrary fractal dimension. The least slope corresponds to Euclidean clusters ( $D = 1$ ), the most one relates to the clusters of the greatest possible coastline dimension, which is equal to the topological dimension of a smooth surface ( $D = 2$ ). Such a fractal dimension is inherent, for example, in Peano curves, which fill the whole plane [28]. Whatever the geometric morphological properties of clusters may be, the slope of their perimeter-area graphs will be always bounded by these two limiting lines.

When we deal with the geometric features of the normal phase clusters, we are considering the cross section of the extended columnar defects by the plane carrying a transport current. Therefore, though normal phase clusters are self-affine fractals [30, 31], it is possible to examine their geometric probability properties in the planar section only, where the boundaries of the clusters are statistically self-similar.

Next, using the relation of Eq. (4) between the fractal perimeter and the area of the cluster, as well as our initial assumption that the critical current of each cluster is inversely proportional to its perimeter, we get the following expression for the critical current:  $I = \alpha A^{-D/2}$ , where  $\alpha$  is the form factor. In accordance with starting formulas of Eq. (1) and Eq. (2), the exponential distribution of cluster areas of Eq. (3) gives rise to an exponential-hyperbolic distribution of critical currents:

$$F(i) = \exp \left[ - \left( \frac{2+D}{2} \right)^{\frac{2}{D}+1} i^{-\frac{2}{D}} \right] \quad (5)$$

where  $i \equiv I/I_c$  is the dimensionless transport current, and  $I_c = \left( \frac{2}{2+D} \right)^{\frac{2+D}{2}} \alpha (\bar{A})^{-\frac{D}{2}}$  is the critical current of the resistive transition.

Thus, the geometric probability properties of the normal phase clusters are responsible for main features of the critical current statistical distribution. In turn, given the distribution of Eq. (5), the change in the trapped magnetic flux caused by the transport current can be found with the aid of Eq. (1). Two of these graphs are displayed in Fig. 2 both for the fractal clusters of coastline dimension  $D = 1.44$  found above (curve (2)) and for the Euclidean ones (curve (3)).

In order to get the relationship between the dynamics of the trapped magnetic flux and geometric morphological properties of the superconducting structure, the sample empirical function  $F^* = F^*(i)$  of the distribution of the critical currents has been computed. This function gives a statistical estimate of the cumulative probability function  $F = F(i)$ . First, the empirical distribution function  $W^* = W^*(A)$  for the primary sampling of the areas of the normal phase clusters has been found. The value  $W^*(A)$  was calculated for each order statistic as the relative number of clusters of area smaller than a given value  $A$ . Next, the empirical distribution of the critical currents was computed for the same order statistics (step line with open circles (1) in Fig. 2) using the following transformations:

$$\left. \begin{aligned} F^* &= 1 - W^* \\ i &= \left( \frac{2+D}{2} \right)^{\frac{2+D}{2}} \left( \frac{\bar{A}}{A} \right)^{\frac{D}{2}} \end{aligned} \right\}$$

Figure 2 shows that in the range of currents  $i < 6$  the empirical distribution function, which describes the morphological properties of the superconducting structure (plot (1)), coincides ideally with the cumulative probability function (curve (2)) for the coastline fractal dimension of  $D = 1.44$ . Starting with the value of the current  $i = 6$  the crossover is observed, resulting in that the empirical distribution function passes to the dependence for Euclidean clusters ( $D = 1$ ). This transition into the Euclidean region is over at large transport currents, when the magnetic flux changes mainly for the breaking of the vortices away from the small clusters (as the smaller clusters have the larger pinning force). The observed crossover has its origin in the finite resolution capability of measuring the cluster geometrical sizes. The distinctive feature of the topologically one-dimensional fractal curve is that its measured length  $P$  depends on the measurement accuracy in such a way:  $P \propto \delta^{1-D}$ , where  $\delta$  is the yardstick size used to measure this length,  $(1 - D)$  is the Hausdorff codimension for the Euclidean 1D-space [28]. In our case such a fractal curve is represented by the boundary of the normal phase cluster. That is why just the statistical distribution of the cluster areas, rather than their perimeters, is fundamental for finding the critical current distribution of Eq. (5). The topological dimension of perimeter is equal to unity and does not coincide with its Hausdorff-Besicovitch dimension, which strictly exceeds the unity. Therefore the perimeter length of a fractal cluster is not well defined, because its value diverges as the yardstick size is reduced infinitely. On the other hand, the topological dimension of the cluster area is the same as the Hausdorff-Besicovitch one (both are equal to two). Thus, the area restricted by the fractal curve is well-defined finite quantity.

Taking into account the effect of the measurement accuracy, the perimeter-area relationship of Eq. (4) can be re-written as

$$P(\delta) \propto \delta^{1-D} (A(\delta))^{\frac{D}{2}} \quad (6)$$

which holds true when the yardstick length  $\delta$  is small enough to measure accurately all boundary of the smallest cluster in sampling. When the resolution is deficient, the Euclidean part of the perimeter length will dominate the fractal one, so there is no way to find the fractal dimension using the scaling relation of Eq. (6). It means that if the length of a fractal curve was measured too roughly with the very large yardstick, its fractal properties could not be detected, and therefore such a geometrical object would be manifested itself as Euclidean one. It is just the resolution deficiency of this kind occurs at the crossover point in Fig. 2. Starting with the cluster area less than  $0.023 \mu\text{m}^2$  (corresponding to the currents of  $i > 6$ ) it is impossible to measure all “skerries” and “fjords” on the cluster coastlines, whereas all the clusters of area less than the size of the measuring cell ( $3.6 \times 10^{-3} \mu\text{m}^2$  that relates to the currents of  $i > 23$ ), exhibit themselves as objects of Euclidean boundaries ( $D = 1$ ). This resolution deficiency can be also observed in Fig. 1: some crosses at its lower left corner are arranged discretely with the spacing equal to the limit of resolution (60 nm), because some marks for smallest clusters coincide for the finite resolution of the picture digitization procedure.

The coastline fractal dimension was found above by means of regression analysis of the whole primary sampling, where the very small clusters of sizes lying at the breaking point of the resolution limit were also included. Therefore, it is necessary to control how much the estimated value of the fractal dimension could be distorted by the presence of such small clusters in that sampling. For this purpose the truncated sampling has been formed in such a way that only 380 clusters of the area greater than  $0.0269 \mu\text{m}^2$ , for which the resolution deficiency is not appeared, have been selected from the primary sampling. The corresponding points are plotted as open circles (2) in Fig. 1, whereas the results of statistical treatment of this truncated sampling are presented in the third column of Table I. The least squares estimation of these perimeter-area data gives the value of coastline fractal dimension  $D = 1.47 \pm 0.03$  with correlation coefficient 0.869. The slope of the regression line for the truncated sampling (dotted line (4) in Fig. 1) is slightly steeper than for the primary one (solid line (3)). It is natural, because the presence in the primary sampling of small clusters, which exhibit themselves as Euclidean ones at the given resolution, leads to underrating the found magnitude of fractal dimension. Nevertheless, the values of fractal dimensions found for both samplings, virtually do not differ within the accuracy of the statistical estimation. This is due to the high robustness of procedure of the fractal dimension estimation on a basis of the scaling relation of Eq. (4): all the points both for the primary sampling and for the truncated one fall on the same straight line, without any bends or breaks (see Fig. 1). At the same time, it is necessary to note, that the empirical distribution function approach (see Fig. 2) provides the most data-sensitive technique of estimating the resolution capability required to study the fractal properties of clusters.

### III. THE PINNING GAIN FOR THE MAGNETIC FLUX TRAPPED IN FRACTALLY BOUNDED CLUSTERS OF A NORMAL PHASE

The found cumulative probability function of Eq. (5) allows us to fully describe the effect of the transport current on the trapped magnetic flux. Using this function, the probability density  $f(i) \equiv dF/di$  for the critical current distribution can be readily derived:

$$f(i) = \frac{2}{D} \left( \frac{2+D}{2} \right)^{\frac{2}{D}+1} i^{-\frac{2}{D}-1} \exp \left[ - \left( \frac{2+D}{2} \right)^{\frac{2}{D}+1} i^{-\frac{2}{D}} \right] \quad (7)$$

This function is normalized to unity over all possible positive values of critical current. The use of the exponential-hyperbolic critical current distribution of Eq. (5) allows us to avoid the inevitable uncertainty caused by truncation of non-physical negative values of depinning currents, as it takes place, for example, in the case of a normal distribution [32]- [34].

The exponential-hyperbolic distribution of Eq. (5) has such an important property: the function  $F = F(i)$  is extremely “flat“ in the vicinity of the co-ordinate origin. It is easy to show that all its derivatives are equal to zero at the point of  $i = 0$ :

$$\frac{d^k}{di^k} F(0) = 0 \quad \text{for any value of } k$$

Therefore even the Taylor series expansion in the vicinity of the origin converges to zero, instead of the quantity  $F$  itself. This mathematical feature has a clear physical meaning: so small transport current does not affect the trapped magnetic flux, because there are no pinning centers of such small critical currents in the overall statistical distribution, so that all the vortices are still too strongly pinned to be broken away. As can be seen from Fig. 2, the change in the magnetic flux becomes appreciable after the transition into a resistive state only (in the transport current range of  $i > 1$ ).

The relative change in the trapped flux  $\Delta\Phi/\Phi$ , which can be calculated from Eq. (5), also defines the density of vortices  $n$  broken away from the pinning centers by the current  $i$ :

$$n(i) = \frac{B}{\Phi_0} \int_0^i f(i') di' = \frac{B}{\Phi_0} \frac{\Delta\Phi}{\Phi} \quad (8)$$

where  $B$  is the magnetic field,  $\Phi_0 \equiv hc/(2e)$  is the magnetic flux quantum ( $h$  is Planck’s constant,  $c$  is the velocity of light,  $e$  is the electron charge). Figure 2 also displays such a practically important property of superconducting structure containing fractal clusters of a normal phase: the fractality intensifies the magnetic flux trapping, hindering its breaking away from pinning centers, and thereby enhances the critical current which sample is capable to withstand, remaining in a superconducting state. Really, the transport current of a magnitude  $i = 2$  causes the 43% of the total trapped magnetic flux to break away from the usual Euclidean clusters (curve (3)), whereas this value is equal only to 25% for fractal normal phase clusters of coastline dimension  $D = 1.44$  (curve (2)). It is equivalent to pinning reinforcement on 73% in the latter case. Thus the pinning amplification due to the fractality can be characterized by the pinning gain factor

$$k_D \equiv \frac{\Delta\Phi(D=1)}{\Delta\Phi(\text{current value of } D)}$$

which is equal to relative decrease in the fraction of magnetic flux broken away from fractal clusters of coastline dimension  $D$  compared to the case of Euclidean ones ( $D = 1$ ). This quantity can be calculated from the following formula:

$$k_D = \exp \left[ \left( \frac{2+D}{2} \right)^{\frac{2}{D}+1} i^{-\frac{2}{D}} - \frac{3.375}{i^2} \right]$$

The characteristic dependencies of the pinning gain on a transport current as well as on fractal dimension are given in Fig. 3. The highest amplification is reached when the cluster boundaries have the greatest possible fractality:  $\max_D k_D = k_2 = \exp((4i - 3.375)/i^2)$ , with the maximum of  $k_2$  at transport current  $i = 1.6875$ . Let us note that the pinning gain characterizes the properties of a superconductor in the range of the transport currents corresponding to a resistive state ( $i > 1$ ). At smaller current the total trapped flux remains unchanged (see Fig. 2) for lack of pinning centers of such small critical currents, so the breaking of the vortices away has not started yet. When a transport current becomes greater than the current of a resistive transition, some finite resistance appears, so that the passage of electric current is accompanied by the energy dissipation. As for any hard superconductor (type-II, with pinning centers) this dissipation does not mean the destruction of phase coherence yet. Some dissipation always accompanies any motion of a magnetic flux that can happen in a hard superconductor even at low transport current. Therefore the critical current in such materials cannot be specified as the greatest non-dissipative current. The superconducting state collapses only when a growth of dissipation becomes avalanche-like as a result of thermo-magnetic instability.

The principal reason of pinning enhancement due to the fractality of the normal phase clusters lies in the fundamental properties of the critical current distribution. Figure 4 demonstrates the peculiarities of the fractal probability density specified by Eq. (7). As in Fig. 1, the thin lines show the extreme cases of Euclidean clusters ( $D = 1$ ) and clusters of boundary with the maximum fractality ( $D = 2$ ). As may be clearly seen from these graphs, the bell-shaped curve of the distribution broadens out, moving towards greater magnitudes of current as the fractal dimension increases. This shift can be described by dependencies of average and mode of the critical current distribution on the fractal

dimension, as it is shown in the inset of Fig. 4. The mode of the distribution, which is equal to the value of the critical current that provides the maximum of the probability density of Eq. (7), depends linearly on the fractal dimension:  $\text{mode } f(i) = (2 + D)/2$ . The average critical current obeys much more strong superlinear law specified by Euler's gamma function:

$$\bar{i} = \left(\frac{2+D}{2}\right)^{\frac{2+D}{2}} \Gamma\left(1 - \frac{D}{2}\right)$$

The mean value of the critical current for Euclidean clusters is equal to  $\bar{i}(D=1) = (3/2)^{3/2} \sqrt{\pi} = 3.2562$ , while for clusters of maximum fractality this value becomes infinite:  $\bar{i}(D=2) \rightarrow \infty$ . Figure 4 clearly demonstrates that increasing the fractal dimension gives a growth of the contribution made by clusters of greater critical current to the overall distribution, resulting just in enhancement of the magnetic flux trapping.

#### IV. ELECTRIC FIELD IN THE RESISTIVE STATE

In the resistive state the hard superconductor is adequately specified by its voltage-current ( $V$ - $I$ ) characteristic. The critical current distribution of Eq. (7) allows us to find the electric field arising from the magnetic flux motion after the vortices have been broken away from the pinning centers. Inasmuch as each normal phase cluster contributes to the total critical current distribution, the voltage across a superconductor  $V = V(i)$  is the response to the sum of effects made by the contribution from each cluster. Such a response can be expressed as a convolution integral:

$$V = R_f \int_0^i (i - i') f(i') di' \quad (9)$$

where  $R_f$  is the flux flow resistance. The similar approach is used universally to consider behavior of the clusters of pinned vortex filaments [35]; to analyze the critical scaling of  $V$ - $I$  characteristics of superconductors [34]; that is to say, in all the cases where the distribution of the depinning currents occurs. The present consideration will be primarily concentrated on the consequences of the fractal nature of the normal phase clusters specified by the distribution of Eq. (7), so all the problems related to possible dependence of the flux flow resistance  $R_f$  on a transport current will not be taken up here.

Let us consider the simplest case, wherein all of the pinning centers would have an identical critical current  $i_c$  so all the vortices would be broken away simultaneously at  $i = i_c$ . Then, referring to Eq. (8), their density would have the following form:

$$n = \frac{B}{\Phi_0} \int_0^i \delta(i' - i_c) di' = \frac{B}{\Phi_0} h(i - i_c)$$

where  $\delta(i)$  is Dirac delta function,

$$h(i) \equiv \begin{cases} 1 & \text{for } i \geq 0 \\ 0 & \text{for } i < 0 \end{cases} \quad \text{is Heaviside step function.}$$

Thus, the trapped flux would change by 100% at once:  $\Delta\Phi/\Phi = h(i - i_c)$ . Let us note that in this case  $i_c = 1$  due to the convenient normalization chosen above:  $i \equiv I/I_c$ .

In the model case of delta-shaped distribution of the critical currents the voltage across a superconductor in the flux flow regime, according to Eq. (9), would obey the simple linear law:  $V = R_f (i - i_c) h(i - i_c)$ . The corresponding  $V$ - $I$  characteristic is shown in Fig. 5 by the dotted line (1).

For fractal distribution of critical currents the situation is quite different, because the vortices are being broken away now in a wide range of the transport currents. After the substitution of the function of Eq. (7) in Eq. (9), upon integration by parts, the voltage across a superconductor can be expressed with the cumulative probability function of Eq. (5):

$$V = R_f \int_0^i F(i') di' \quad (10)$$

integration of which gives:

$$V = R_f \exp\left[-\left(\frac{2+D}{2}\right)^{\frac{2}{D}+1} i^{-\frac{2}{D}}\right] \left\{ i - \left(\frac{2+D}{2}\right)^{\frac{2+D}{2}} U\left[\frac{D}{2}, \frac{D}{2}, \left(\frac{2+D}{2}\right)^{\frac{2}{D}+1} i^{-\frac{2}{D}}\right] \right\} \quad (11)$$

where  $U(a, b, z)$  is Tricomi confluent hypergeometric function.

In extreme cases for  $D = 1$  and for  $D = 2$  expression of Eq. (11) can be simplified (see Appendix):

(a) Euclidean clusters ( $D = 1$ ):

$$V = R_f \left[ i \exp\left(-\frac{3.375}{i^2}\right) - \sqrt{3.375\pi} \operatorname{erfc}\left(\frac{\sqrt{3.375}}{i}\right) \right] \quad (12)$$

where  $\operatorname{erfc}(z)$  is the complementary error function.

(b) Clusters of boundary with the maximum fractality ( $D = 2$ ):

$$V = R_f \left[ i \exp\left(-\frac{4}{i}\right) + 4 \operatorname{Ei}\left(-\frac{4}{i}\right) \right] \quad (13)$$

where  $\operatorname{Ei}(z)$  is the exponential integral function.

The  $V$ - $I$  characteristics of a superconductor containing fractal normal phase clusters are presented in Fig. 5. All the curves are virtually starting with the transport current value of  $i = 1$  that is agreed with the onset of the resistive state found above from cumulative probability function of Eq. (5). When the current increases the trapped flux remains unchanged until the vortices start to break away from the pinning centers. As long as the magnetic flux does not move, no electric field is arisen. Two thin lines (2), calculated using the formulas of Eq. (12) and Eq. (13), bound the region the  $V$ - $I$  characteristics can fall within for any possible values of fractal dimension. As an example, the curve (3) demonstrates the  $V$ - $I$  characteristic of a superconductor containing fractal clusters of previously obtained coastline dimension  $D = 1.44$ . This figure shows that the fractality reduces appreciably an electric field arising from the magnetic flux motion. This effect is especially strong in the range of the currents  $1 < i < 3$ , where the pinning enhancement also has a maximum (see Fig. 3). Both these effects have the same nature, inasmuch as their reason consists in the peculiarities of fractal distribution of critical currents of Eq. (7). As is seen from Fig. 4, an increase of fractality causes a significant broadening of the tail of the distribution  $f = f(i)$ . It means that more and more of small clusters, which can best trap the magnetic flux, are being involved in the game. Hence the density of vortices broken away from pinning centers by the Lorentz force is reducing, so the smaller part of a magnetic flux can flow, creating the smaller electric field. In turn, the smaller the electric field is, the smaller is the energy dissipated when the transport current passes through the sample. Therefore, the decrease in heat-evolution, which could cause transition of a superconductor into a normal state, means that the current-carrying capability of the superconductor containing such fractal clusters is enhanced.

Thus, Fig. 5, as well as Fig. 3, obviously demonstrates such a practically important result: the fractality of the boundary of the normal phase clusters, which act as the pinning centers, prevents the destruction of a superconductivity by a transport current, and therefore, causes the critical current to increase.

## V. CONCLUSION

Thus, the fractal properties of the normal phase clusters have an essential influence on the dynamics of the trapped magnetic flux. The crucial change of the critical current distribution caused by increasing of the coastline fractal dimension of the normal phase clusters forms the basis of this effect. The most important result is that the fractality of cluster boundary strengthens the flux pinning and thereby hinders the destruction of superconductivity by the transport current, resulting in enhancement of the current-carrying capability of a superconductor. This phenomenon provides the principally new possibilities for increasing the critical current value of composite superconductors by optimizing their geometric morphological properties.

### APPENDIX A: ELECTRIC VOLTAGE ACROSS A SUPERCONDUCTOR CAUSED BY THE MAGNETIC FLUX MOTION IN EXTREME CASES OF EUCLIDEAN CLUSTERS AND CLUSTERS OF MAXIMUM FRACTALITY

In order to obtain the expressions of Eq. (11) - Eq. (13) for the voltage across a superconductor, it is necessary to integrate the cumulative probability function for the critical current distribution of Eq. (5). The substitution of exponential-hyperbolic distribution of Eq. (5) in Eq. (10) gives:

$$\frac{V}{R_f} = \int_0^i dx \exp\left(-Cx^{-\frac{2}{D}}\right) \quad , \quad \text{where} \quad C \equiv \left(\frac{2+D}{2}\right)^{\frac{2}{D}+1} \quad (A1)$$

Using the change of a variable of the form  $y \equiv Cx^{-2/D}$ , we can get the following expression:

$$\frac{V}{R_f} = \frac{D}{2} C^{\frac{D}{2}} \int_{C i^{-\frac{2}{D}}}^{\infty} dy e^{-y} y^{-\frac{2+D}{2}}$$

which, upon integration by parts, becomes:

$$\frac{V}{R_f} = i \exp\left(-C i^{-\frac{2}{D}}\right) - C^{\frac{D}{2}} \Gamma\left(1 - \frac{D}{2}, C i^{-\frac{2}{D}}\right) \quad (\text{A2})$$

where  $\Gamma(\nu, z) \equiv \int_z^{\infty} dy e^{-y} y^{\nu-1}$  is the incomplete gamma function. This function can be represented as:

$$\Gamma(\nu, z) = e^{-z} U(1 - \nu, 1 - \nu, z) \quad (\text{A3})$$

where  $U(a, b, z) \equiv (\Gamma(a))^{-1} \int_0^{\infty} dy e^{-zy} y^{a-1} (1+y)^{b-a-1}$  is Tricomi confluent hypergeometric function; and  $\Gamma(a) \equiv \int_0^{\infty} dy e^{-y} y^{a-1}$  is Euler gamma function.

Thus with the help of Eq. (A3), the expression for the voltage across a superconductor of Eq. (A2) can be written in its final form:

$$\frac{V}{R_f} = \exp\left(-C i^{-\frac{2}{D}}\right) \left[ i - C^{\frac{D}{2}} U\left(\frac{D}{2}, \frac{D}{2}, C i^{-\frac{2}{D}}\right) \right] \quad (\text{A4})$$

This formula is similar to the expression of Eq. (11). The corresponding  $V$ - $I$  characteristic of a superconductor calculated using this expression at  $D = 1.44$  is shown in Fig. 5 by the curve (3).

The equation (A4) can be transformed to more simple form in two special cases:

(a) For clusters of Euclidean boundary ( $D = 1$ ):

At  $D = 1$  the following representation is valid for Tricomi confluent hypergeometric function:

$$U\left(\frac{1}{2}, \frac{1}{2}, z\right) = \sqrt{\pi} e^z \operatorname{erfc}(\sqrt{z})$$

where  $\operatorname{erfc}(z) \equiv (2/\sqrt{\pi}) \int_z^{\infty} dy e^{-y^2}$  is the complementary error function.

The substitution of this representation into the equation (A4) gives the same expression for the voltage across a superconductor as the formula of Eq. (12):

$$\frac{V}{R_f} = i \exp\left(-\frac{C}{i^2}\right) - \sqrt{\pi C} \operatorname{erfc}\left(\frac{\sqrt{C}}{i}\right) \quad (\text{A5})$$

where, according to Eq. (A1),  $C = 3.375$ .

(b) For clusters of boundary with the maximum fractality ( $D = 2$ ):

At  $D = 2$  there is such a representation for Tricomi confluent hypergeometric function:

$$U(1, 1, z) = -e^z \operatorname{Ei}(-z)$$

where  $\operatorname{Ei}(-z) \equiv \int_{-\infty}^{-z} dy \frac{e^y}{y}$ ,  $z > 0$ , is the exponential integral function.

Taking into account this formula, the expression (A4) for the voltage across a superconductor can be re-written as:

$$\frac{V}{R_f} = i \exp\left(-\frac{C}{i}\right) + C \operatorname{Ei}\left(-\frac{C}{i}\right) \quad (\text{A6})$$

where, according to Eq. (A1),  $C = 4$ . The last formula coincides with the expression of Eq. (13).

The formulas of Eqs. (A5), (A6) describe dependencies of the voltage across a superconductor in a resistive state on the transport current for extreme values of the coastline fractal dimension. Two corresponding  $V$ - $I$  curves are shown in Fig. 5 by thin lines (2). Whatever the geometric morphological properties of the normal phase clusters may be, the  $V$ - $I$  characteristics of a superconductor will fall within the region bounded by those two limiting curves, as it is shown in Fig. 5 (like the curve (3) drawn for  $D = 1.44$ ).

- 
- [1] T. Higuchi, S. I. Yoo, M. Murakami, Phys. Rev. B **59**, 1514 (1999).
- [2] Ch. Jooss, R. Warthmann, H. Kromüller, T. Haage, H.-U. Habermeier, J. Zegenhagen, Phys. Rev. Lett. **82**, 632 (1999).
- [3] L. Krusin-Elbaum, G. Blatter, J. R. Thompson, D. K. Petrov, R. Wheeler, J. Ullmann, C. W. Chu, Phys. Rev. Lett. **81**, 3948 (1998).
- [4] S. N. Dorogovtsev, Yu. I. Kuzmin, Phys. Lett. A **170**, 245 (1992).
- [5] R. Surdeanu, R. J. Wijngaarden, B. Dam, J. Rector, R. Griessen, C. Rossel, Z. F. Ren, J. H. Wang, Phys. Rev. B **58**, 12467 (1998).
- [6] E. Mezzetti, R. Gerbaldo, G. Ghigo, L. Gozzelino, B. Minetti, C. Camerlingo, A. Monaco, G. Cuttone, A. Rovelli, Phys. Rev. B **60**, 7623 (1999).
- [7] M. R. Beasley, Artificially-Structured Superconductors. - In: Percolation, Localization and Superconductivity (ed. by A. M. Goldman and S. A. Wolf, NATO ASI Series, Ser.B, vol.109, Plenum Press, New York, 1984), pp.115-143.
- [8] R. B. Laibowitz, R. F. Voss, E. I. Alessandrini, Clustering in Thin Au Films Near the Percolation Threshold. - In: Percolation, Localization and Superconductivity (ed. by A. M. Goldman and S. A. Wolf, NATO ASI Series, Ser.B, vol.109, Plenum Press, New York, 1984), pp.145-160.
- [9] C. J. Olson, C. Reichhardt, F. Nori, Phys. Rev. Lett. **80**, 2197 (1998).
- [10] Yu. I. Kuzmin, Phys. Lett. A **267**, 66 (2000).
- [11] L. Krusin-Elbaum, L. Civale, G. Blatter, A. D. Marwick, F. Holtzberg, C. Feild, Phys. Rev. Lett. **72**, 1914 (1994).
- [12] D. R. Nelson, V. M. Vinokur, Phys. Rev. B **48**, 13060 (1993).
- [13] Yu. I. Kuzmin, I. V. Plechakov, Tech. Phys. Lett. **25**, 475 (1999).
- [14] Yu. I. Kuzmin, I. V. Pleshakov, S. V. Razumov, Phys. Solid State **41**, 1594 (1999).
- [15] D. Stauffer, Phys. Reports **54**, 2 (1979).
- [16] G. Blatter, M. V. Feigel'man, V. B. Geshkenbein, A. I. Larkin, V. M. Vinokur, Rev. Mod. Phys. **66**, 1125 (1994).
- [17] X. Y. Cai, A. Gurevich, I-Fei Tsu, D. L. Kaiser, S. E. Babcock, D. C. Larbalestier, Phys. Rev. B **57**, 10951 (1998).
- [18] D. J. Scalapino, Phys. Reports **250**, 329 (1995).
- [19] M. J. M. E. De Nivelle, G. J. Gerritsma, H. Rogalla, Phys. Rev. Lett. **70**, 1525 (1993).
- [20] H. Pastoriza, S. Candia, G. Nieva, Phys. Rev. Lett. **83**, 1026 (1999).
- [21] H. Küpfer, Th. Wolf, A. A. Zhukov, R. Meier-Hirmer, Phys. Rev. B **60**, 7631 (1999).
- [22] H. R. Kerchner, D. P. Norton, A. Goyal, J. D. Budai, D. K. Christen, D. M. Kroeger, M. Paranthaman, D. F. Lee, F. A. List, R. Feenstra, E. H. Brandt, Phys. Rev. B **60**, 6878 (1999).
- [23] V. V. Bryksin, A. V. Goltsev, S. N. Dorogovtsev, Yu. I. Kuzmin, A. N. Samukhin, J. Phys.: Condens. Matter **4** 1791 (1992).
- [24] R. Haslinger, R. Joynt, Phys. Rev. B **61**, 4206 (2000).
- [25] A. I. Rykov, S. Tajima, F. V. Kusmartsev, E. M. Forgan, Ch. Simon, Phys. Rev. B **60**, 7601 (1999).
- [26] I. Maggio-April, C. Renner, A. Erb, E. Walker, O. Fisher, Nature **390**, 487 (1997).
- [27] J. E. Sonier, R. F. Kiefl, J. H. Brewer, D. A. Bonn, S. R. Dunsiger, W. N. Hardy, R. Liang, R. I. Miller, D. R. Noakes, C. E. Stronach, Phys. Rev. B **59**, R729 (1999).
- [28] B. B. Mandelbrot, Fractals: Form, Chance, and Dimension (Freeman, San Francisco, 1977).
- [29] B. B. Mandelbrot, The Fractal Geometry of Nature. (Freeman, San Francisco, 1982).
- [30] B. B. Mandelbrot, Self-Affine Fractal Sets. - In: Fractals in Physics (ed. by L. Pietronero and E. Tosatti, North-Holland, Amsterdam, 1986) pp.3-28.
- [31] J. Feder, Fractals (Plenum Press, New York, 1988).
- [32] Yu. I. Kuzmin, A. P. Paugurt, I. V. Pleshakov, S. V. Rasumov, Supercond. Science and Technol. **7**, 41 (1994).
- [33] R. Wördenweber, Phys. Rev. B **46**, 3076 (1992).
- [34] B. Brown, Phys. Rev. B **61**, 3267 (2000).
- [35] W. H. Warnes, D. C. Larbalestier, Appl. Phys. Lett. **48**, 1403 (1986).

---

Primary sampling	Truncated sampling
------------------	--------------------

Sampling size	528	380
Mean $A$ , $\mu\text{m}^2$	0.0765	0.1002
Sample standard deviation of $A$ , $\mu\text{m}^2$	0.0726	0.0729
Standard error of estimate for $A$ , $\mu\text{m}^2$	$3.16 \times 10^{-3}$	$3.74 \times 10^{-3}$
Total scanned $A$ , $\mu\text{m}^2$	40.415	38.093
Min value of $A$ , $\mu\text{m}^2$	$2.07 \times 10^{-3}$	0.0269
Max value of $A$ , $\mu\text{m}^2$	0.4015	0.4015
Mean $P$ , $\mu\text{m}$	1.293	1.616
Sample standard deviation of $P$ , $\mu\text{m}$	0.962	0.949
Standard error of estimate for $P$ , $\mu\text{m}$	0.0419	0.0487
Total scanned $P$ , $\mu\text{m}$	682.87	614.19
Min value of $P$ , $\mu\text{m}$	0.096	0.515
Max value of $P$ , $\mu\text{m}$	5.791	5.791
Correlation coefficient	0.929	0.869
Estimated fractal dimension $D$	1.44	1.47
Standard deviation of $D$	0.02	0.03

TABLE I. Statistics of normal phase clusters and estimation of fractal dimension

FIG. 1. Perimeter-area relationship for the normal phase clusters with fractal boundary. Plot (1) shows the data of the primary sampling (528 points); plot (2) shows the data of the truncated sampling (380 points); line (3) is the least square regression line for the primary sampling; line (4) is the least square regression line for the truncated sampling. Two lines (5) display the range of slope that the perimeter-area curves can have for any possible fractal dimension  $D$ . ( $D = 1$  - for clusters of Euclidean boundary,  $D = 2$  - for clusters of boundary with the maximum fractality).

FIG. 2. Effect of a transport current on the magnetic flux trapped in fractal clusters of a normal phase. Step line with open circles (1) is the sample empirical function of critical current distribution; line (2) shows the decrease in trapped flux for the fractal clusters of coastline dimension  $D = 1.44$ ; line (3) shows the decrease in trapped flux for Euclidean clusters of coastline dimension  $D = 1$ .

FIG. 3. Pinning gain for an arbitrary coastline fractal dimension of the cluster perimeter.

FIG. 4. Influence of the fractal dimension of the perimeter of the normal phase clusters on the critical current distribution. The inset shows the dependencies of the average critical current  $\bar{i}$  and mode  $mode f(i)$  of this distribution on the coastline fractal dimension.

FIG. 5. Voltage-current characteristics of superconductors containing fractal clusters of a normal phase. Dotted line (1) corresponds to the delta-shaped distribution of the critical currents; lines (2) - to extreme dependencies of the voltage across a superconductor on the transport current in the case of Euclidean clusters ( $D = 1$ ) and clusters of boundary with the maximum fractality ( $D = 2$ ); line (3) - to  $V$ - $I$  characteristic of superconductor containing the normal phase clusters of fractal dimension of the perimeter  $D = 1.44$ .

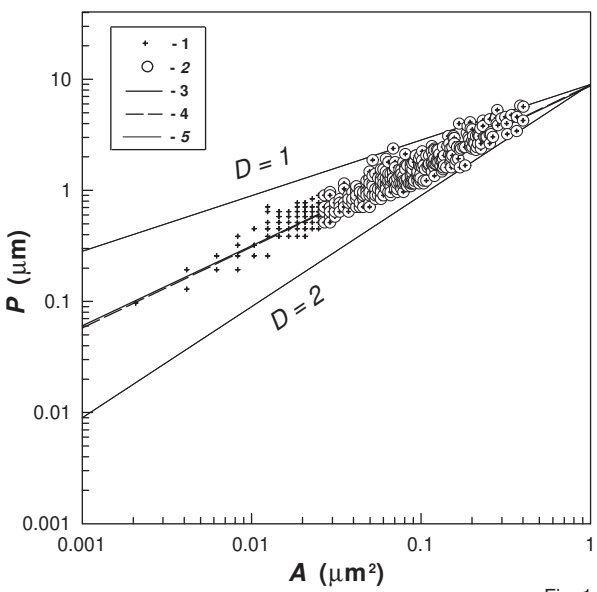


Fig. 1

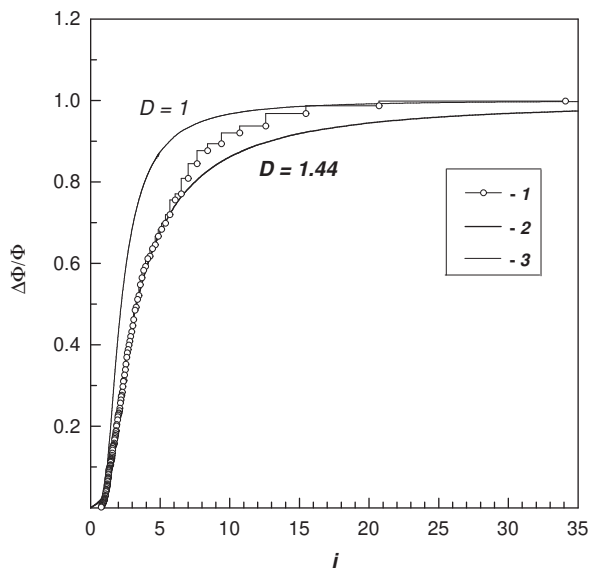


Fig. 2

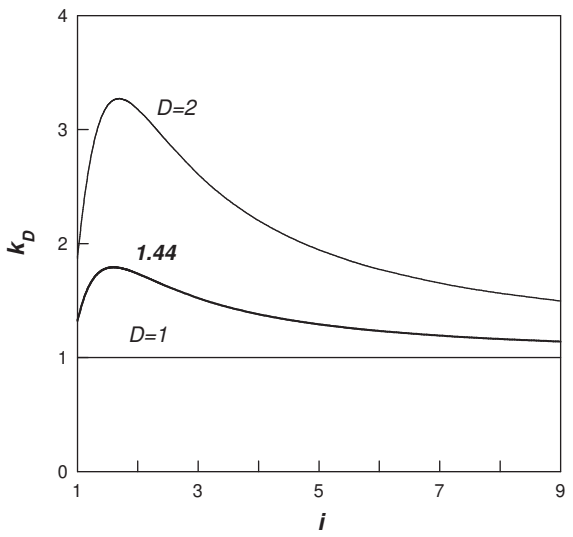


Fig. 3

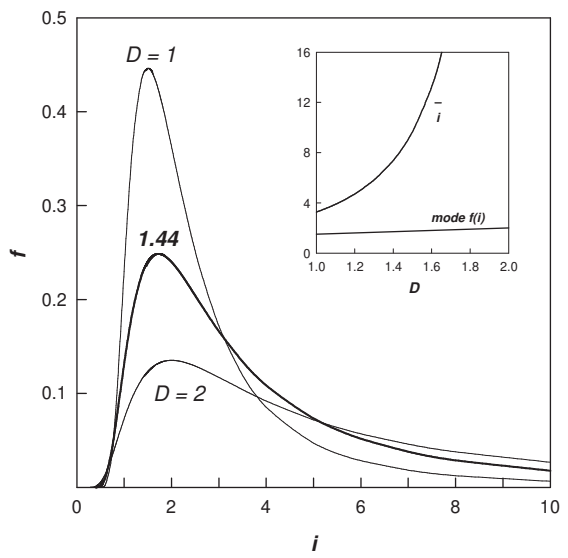


Fig. 4

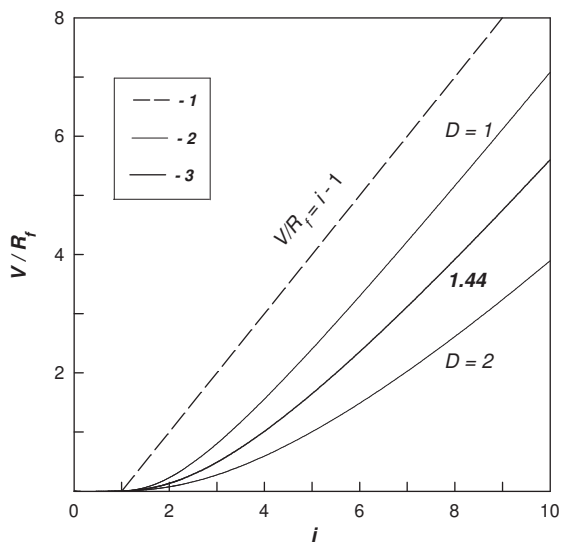


Fig. 5